Nanoscale zero-valent iron supported on carbon nanotubes for polychlorinated biphenyls removal

Xiuqin Cao[a,*], Haoran Wang[b], Chunmiao Yang[b], Lin Cheng[b], Kunming Fu[a], Fuguo Qiu[a]

[a]*Key Laboratory of Urban Storm Water System and Water Environment, Ministry of Education, Beijing University of Civil Engineering and Architecture; School of Environment and Energy Engineering, Beijing University of Civil Engineering and Architecture, No. 1 Zhanlanguan Road, Xicheng District, Beijing 100044, China, emails: caoxiuqin@bucea.edu.cn (X. Cao), fukunming@bucea.edu.cn (K. Fu), qiufuguo@bucea.edu.cn (F. Qiu)*
[b]*School of Environment and Energy Engineering, Beijing University of Civil Engineering and Architecture, No. 1 Zhanlanguan Road, Xicheng District, Beijing 100044, China, emails: 13051517936@163.com (H. Wang), cmyang77@126.com (C.Yang), 917151363@qq.com (L. Cheng)*

ABSTRACT

Nanoscale zero-valent iron (nZVI)-multiwalled carbon nanotube (MWCNT) was first applied to remove polychlorinated biphenyls (PCBs) from water. The characterization result from scanning electron microscopy, transmission electron microscopy, and X-ray powder diffraction showed that the nZVI was immobilized successfully on the surface or into the network of MWCNTs. The effects of different reaction conditions like temperature, initial pH values, MWCNT-nZVI dosage, and initial PCBs concentrations for the removal of PCBs were evaluated. Comparing to pure nZVI or MWCNT, the MWCNT-nZVI nanocomposites exhibited around 30% higher efficiency on PCBs removal. The removal process obeyed the pseudo-secondary-order kinetics model. By calculating the material balance of Cl^- during the degradation of PCBs by MWCNT-nZVI, it demonstrated that MWCNT-nZVI has not only a reducing effect but also an adsorption effect on PCBs. During the reaction, reduction plays a dominant role. The reductive activity of nZVI was efficiently supported by MWCNT, which can accelerate electrons transfer in the composite and greatly enhance the reduction activity of nZVI. At the same time, the reusability and stability of MWCNT-nZVI were considered. Overall, MWCNT-nZVI nanocomposites offer a promising alternative material for the removal of PCBs from water.

Keywords: Nanoscale zero-valent iron; Carbon nanotubes; PCBs; Influence factors; Dechlorination

1. Introduction

Polychlorinated biphenyls (PCBs) are one of the 12 priorities controlled persistent organic pollutants (POPs) in the Stockholm Convention issued in 2001. PCBs are mixtures of up to 209 individual chlorinated compounds containing a different number of chlorine atoms per molecule known as congeners. According to the substitution position of the chlorine atom on the benzene ring, there are theoretically 209 different PCBs, which are widely distributed in the environment [1–3]. PCBs were first synthesized in 1927. Because of its excellent performance, it was commonly

* Corresponding author.

used in dielectrics and coolants for electrical instruments, plasticizers for coatings, rubber sealants, and in the power industry, chemical, plastics, and printing industries [4–6]. Depending on the statistics, it has been estimated that global production since that time is of the order of 10^6 tons [7]. Some studies have shown that PCBs can accumulate in the tissues of aquatic animals and plants, eventually gathering in the human through the food chain, and causing many adverse effects, including resisting metabolism in vertebrate species metabolism, DNA damage and increasing the risk of carcinogenesis [8–10]. Owning to their bioaccumulation and resistance to biodegradation, if it was released into the water supply system, it will pose a serious threat to the environment and public health [11]. At the same time, urban areas under the influence of multi-industrial activities with arid and semi-arid environments witness a significant increase in environmental pollution, especially in the water sector. Many physio-chemical and biological parameters and metal especially arsenic were exceeding the permissible limit of Punjab environmental quality standards and the World Health Organization [12–14].

Numerous researchers have been working on exploring efficient and simple PCBs degradation methods in recent decades [15,16]. Bioremediation approaches that include the use of plants and microbial communities to promote the degradation of PCB have significant potential. Wang et al. [17] cultivated and characterized two *Dehalococcoides mccartyi* strains (CG3 and SG1), and revealed interspecies synergistic interactions in PCB-dechlorinating microbial communities via mutagenesis analysis. Xu et al. [18] studied the effects of alfalfa growth and inoculation with symbiotic nitrogen-fixing bacteria (rhizobia) on the removal of PCBs from rhizosphere soil through field experiments. After planting for 90 d, the PCB removal for the rhizosphere soil was enhanced in the planted treatments, With an initial PCB content of 414 to 498 μg/kg in the soil, the PCB content decreased by an average of 36%, while the unplanted soil decreased by 5.4%. Bioremediation will take more time to grow the strain and complete dechlorination [19]. Considering polyethylene (micro-PE), 70 nm polystyrene (nano-PS), multi-walled carbon nanotubes (MWCNT), and fullerene (C60) to adsorb PCBs and organics (OM), the results showed that PCBs The adsorption rate of C60 is 3–4 orders of magnitude stronger than that of OM and micro-PE. Sorption to nano-PS was 1−2 orders of magnitude stronger than to micro-PE, which was attributed to the higher aromaticity and surface−volume ratio of nano-PS [20]. Shao et al. [21] suggested that the β-CD grafted MWCNTs (MWCNT-g-CD) had much higher adsorption capacity than MWCNTs in the removal of PCBs from aqueous solutions. MWCNT-g-CD reached adsorption equilibrium for PCBs in 50 h, and the maximum adsorption capacity is 240 mg/g. Due to the pollutants are not completely eliminated, and it is difficult to regenerate the adsorbent. The method of physical adsorption is gradually going out of favor. Chemically treated PCBs mainly use oxidation and reduction methods. Dudasova et al. [22] reported that the removal of polychlorinated biphenyl congeners in mixture Delor 103 from wastewater by ozonation vs./and biological method. Results showed that 86% of the total amount of the nine selected PCB congeners (PCB 8, 28, 52, 101, 118, 153,

138, 180, and 203) were removed by the ozonation method. However, based on energy consumption and remediation efficiency, reductive methods have emerged as being advantageous for remediation of PCBs [23]. Liu and Zhang [24] studied that the composite nano-zero valent iron (nZVI) contained in porous carbon (PC/nZVI) achieved more than 90% degradation of PCBs within 16 h. In a word, chemical extraction, oxidation/reduction, dehalogenation are the most effective, economic and non-toxic ways to remove the PCBs in the liquid-phase [22].

Zero valent iron (ZVI) or elemental iron (Fe^0) has been studied as a cost-effective technology for the remediation of environmental contaminants since the early 1990s [25,26]. Because of its small particle size, large specific surface area, high reaction surface sites, and high reactivity, and reaction conditions, nanoscale zero-valent iron (nZVI) is often used to treat halogenated organic compounds in wastewater and groundwater, which is a new environmental remediation technology [25]. However, it suffered from many shortcomings when nZVI was applied in practical engineering. Firstly, nZVI has strong magnetic properties, easy agglomeration, and poor mechanical strength, poor dispersion in water [27], which is easy to be oxidized by air and forms an oxide layer that blocks the serviceable active surface sites [28]. At the same time, it has some environmental health risks and needs to control [29]. To overcome the challenges in practical engineering, in recent years, a suitable material has been adopted to develop mechanical support of nZVI to enhance its dispersion performance [30]. Carbon nanotubes (CNT) [31,32] have a large specific surface area, small particle size, strong adsorption capacity, qualities of low cost, and adsorb strongly toward PCBs [20], which has been tested as select supports to inhibit the aggregation of nZVI particles and hence increase the reaction performance. Lv et al. [33] adopted nanoscale Nanoscale zero-valent (nZVI)-multi-walled carbon nanotube (MWCNT) nanocomposites firstly to remove Cr(VI) from wastewater. In this paper, a multi-walled carbon nanotube was used as a porous-based support material for synthesizing nZVI. More recently, nZVI supported by natural bentonite (B-nZVI) and stabilized by polypyrrole/attapulgite has been reported to increase the durability and mechanical strength of nZVI. Soliemanzadeh and Fekri [34] reported that the synthesis of nanoscale zero-valent iron (nZVI) in the presence of natural bentonite (B-nZVI) using green tea extract, and suggests that B-nZVI could be used as a suitable adsorbent for the removal of phosphorus from aqueous solutions. Chen et al. [35] had been successfully synthesized polypyrrole/attapulgite-supported nanoscale zero-valent iron (PPy/APT-nZVI), investigating the composites PPy/APT-nZVI to extract Naphthol green B (NGB) from aqueous solution. However, only a few studies have reported using MWCNT as support materials for nZVI [33].

In this study, multiwalled carbon nanotubes (MWCNTs) were selected as support material for the nZVI to synthesis MWCNT-nZVI by liquid-phase reduction. The objectives of this paper were: (1) to prepare MWCNT-nZVI and characterize by scanning electron microscopy (SEM), transmission electron microscopy (TEM), powder X-ray diffraction (PXRD), and Brunauer–Emmett–Teller (BET), (2)

to investigate the effecting factors the PCBs removal efficiency by MWCNT-nZVI, including the temperature, pH, initial PCBs concentration, and MWCNT-nZVI dosage, (3) to research the kinetics and thermodynamics model fitting with PCBs removal by MWCNT-nZVI, and kinetic and thermodynamic analyses were used to study the reduction process, and possible mechanism of PCBs removal was discussed. This study was expected to provide a theoretical basis of MWCNT-nZVI future applications of water pollution control.

2. Materials and methods

2.1. Reagents

Ferrous sulfate heptahydrate (FeSO$_4$·7H$_2$O, analytical reagent (AR)), sodium borohydride (NaBH$_4$, AR), ethyl alcohol (AR), acetone (AR), *n*-hexane (AR), isopropanol (AR), MWCNTs (purity > 98%, diameter of 20–30 mm, length of 10–30 μm, surface area >110 m^2/g, density of 0.22 g/cm^3). All of them were purchased from Beijing DK nano technology Co., Ltd. PCBs (PCB28, PCB52, PCB101, PCB118, PCB138, PCB153, and PCB180 were purchased from Accustandard Inc., (New Haven USA). The general characteristics of studying PCBs were shown in Table 1. The experimental water is deionized water, which was used throughout experiments from a Millipore Milli-Q system (18.2 MΩ/cm).

2.2. Preparation of MWCNT-nZVI
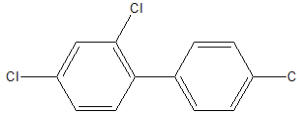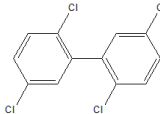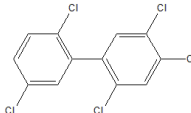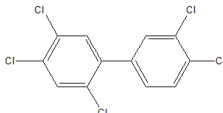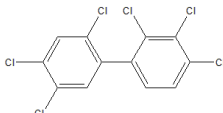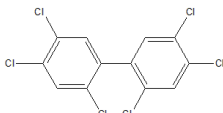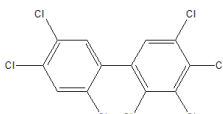
The MWCNT-nZVI were prepared by the liquid precipitation method (Eq. 1) [36]:

$$Fe^{2+} + 2BH_4^- + 6H_2O \rightarrow Fe^0 + 2B(OH)_3 + 7H_2 \uparrow \qquad (1)$$
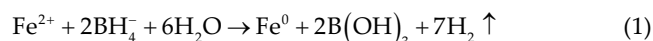
Ten grams of MWCNTs were heated in ultrapure water for 30 min to remove some impurities and dried in a constant temperature oven for 24 h. 2.48 g of FeSO$_4$·7H$_2$O were dissolved in 100 mL acetone/ultra-pure water (V_1:V_2 = 2:3), MWCNTs (10 g) were mixed in 100 mL FeSO$_4$·7H$_2$O/acetone/ultra-pure solution, the mixture was transferred into 500 mL four neck flasks. Two hundred and fifty milliliters of NaBH$_4$ (1 mol/L) as a reducing agent and were added drop by drop to a four-necked flask by peristaltic pump

Table 1
General characteristics of the studied PCBs

Name	Structure	Molecular weight (g/mol)
2,4,4′-Trichlorobiphenyl (PCB 28)		257.5
2,2′,5,5′-Tetrachlorobiphenyl (PCB 52)		292.0
2,2′,4,5,5′-Pentachlorobiphenyl (PCB 101)		326.4
2,3′,4,4′,5-Pentachlorobiphenyl (PCB 118)		326.4
2,2′,3,4,4′,5′-Hexachlorobiphenyl (PCB 138)		360.8
2,2′,4,4′,5,5′-Hexachlorobiphenyl (PCB 153)		360.8
2,2′,3,4,4′,5,5′-Heptachlorobiphenyl (PCB 180)		395.3

controlled. Add NaOH solution to adjust to 4.0, and stirring until the reaction had no obvious bubble generation. The whole reduction process continued to flush into nitrogen to maintain the anaerobic environment in the four neck flasks. The preparation route of MWCNT-nZVI is illustrated in Fig. 1.

The MWCNT-nZVI was separated by conventional centrifugation and washed by acetone, *n*-hexane, and ultra-pure water one by one. MWCNT-nZVI were freeze-dried for 18 h and kept in a nitrogen atmosphere to avoid oxidation. All samples of the experiment were synthesized as soon as possible before use.

2.3. Characterization and analysis methods

The surface morphology and particle size of the MWCNT-nZVI and MWCNT were studied by the (Carl-Zeiss, Oberkochen, Germany) and TEM. PXRD patterns were recorded in the range of 2θ = 20°–80° on a DX-2700B X-ray diffractometer with Cu Kα radiation to investigate the elemental composition. The BELSORP-max (BET) was applied to analyze the surface area and pore size of MWCNT-nZVI. The pH meter was applied to measure the pH values. The chloride ion concentration was determined by ICS-1000 ion chromatography (IC, DIONEX, USA).

The PCBs were determined by a gas chromatograph/mass spectrometer (GC–MS, QP2010, Shimadzu Corporation, Japan) added with a DB-5MS column (30 mm × 0.25 mm × 0.25 μm). Chromatographic conditions: the carrier gas was He at 1 mL/min. The oven temperature gradient was designed: start with an initial oven temperature of 100°C for 1 min, ramp rate of 30°C/min, and final temperature of 280°C for 10 min, the sample volume is 10 μL. Mass spectrometry condition: electron bombardment ion source (EI, 70 eV), ion source temperature is 260°C, Interface temperature is 280°C.

2.4. Batch experiments

Isopropanol solution (Wt = 10%) is used as the dispersing agent, to investigate the impacts on PCBs removal reaction by MWCNT-nZVI though batch experiment. PCBs with a concentration and material (MWCNT, MWCNT-nZVI) were added into 100 mL reaction bottles, and double sealed with Teflon butyl stopper and aluminum cover. To reduce the errors, each of the experiments has been repeated twice. Aliquots of the samples were taken at certain time intervals, and samples were added with 1 mL of *n*-hexane and extracted for 4 h in an oscillator, then the PCBs analysis was carried out by GC-MS. The PCBs were adsorbed by MWCNT-nZVI/ MWCNT, which was extracted by Soxhlet extraction apparatus and determined using GC-MS. After the vacuum filtered, the solution passes through the solid-phase extraction cartridge then the concentration of Cl$^-$ in the solution is determined by ion chromatography.

To compare the removal performance, MWCNT and MWCNT-nZVI were applied in PCBs removal. The optimum reaction conditions including pH, temperature, MWCNT-nZVI dosage, and initial PCBs concentrations were verified. Initial temperature ranged from 15°C, 20°C, 25°C, 30°C, and 35°C, initial MWCNT-nZVI dosages were set for 1.0, 1.2, 1.4, 1.6, and 2.0 g/L, while different initial pH values were 3.0, 5.0, 7.0, 8.5, and 10.0, initial PCBs concentrations were investigated for 0.7, 1.4, 2.1, and 2.8 mg/L, respectively. Through the batch experiments above, the optimal removal conditions were obtained.

3. Results and discussion

3.1. Characterization of MWCNT-nZVI

3.1.1. SEM and TEM characterization

The morphologies and surface of MWCNT and MWCNT-nZVI were shown in Fig. 2, the diameter of MWCNT in 20–30 nm and smooth surface are presented in Fig. 2a, and there were numerous bright and clear spherical spots in Fig. 2c. Several researchers have reported that the bright spherical spots are nZVI particles (the diameter in 20–80 nm) [33,37], Previous studies have reported that non-supported nZVI particles were linked as a neck-lace-like chain and grew rapidly to form microspheres [38]. The aggregation is attributed to the combined effect of the
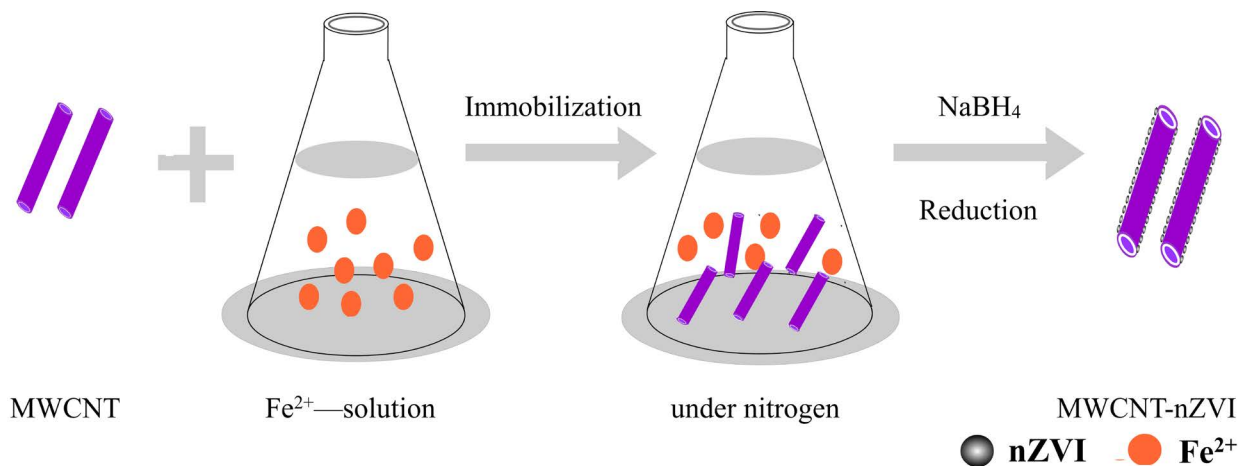

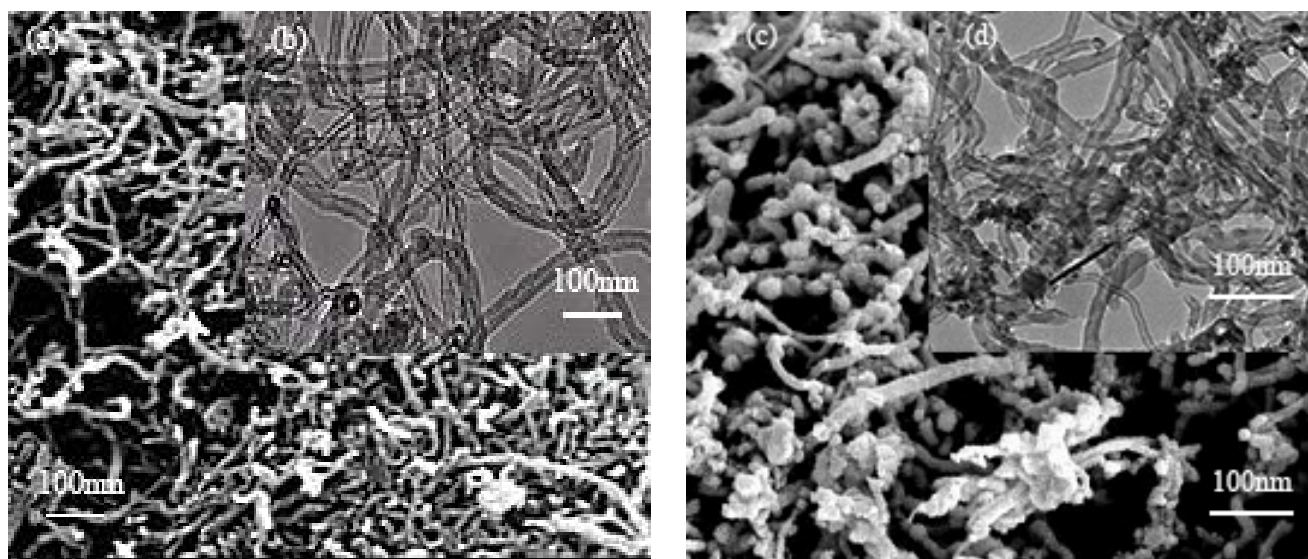Fig. 1. Preparation route of MWCNT-nZVI composites.

Fig. 2. (a) SEM images of MWCNT, (b) TEM images of MWCNT, (c) SEM images of MWCNT-nZVI, and (d) TEM images of MWCNT-nZVI.

magnetic properties of nZVI [39–41]. Aggregation of nZVI particles was still observed from Fig. 1c, but much decreased relative to the unsupported nZVI nanoparticles [42,43]. As shown in Figs. 2c and d, the clear nZVI particles (perfect black round) located on the surface or inside the network of MWCNTs. The structural characteristics of MWCNT-nZVI can increase the specific surface area of nZVI, overcome the aggregation and passivation of nZVI, and improve the stability of the reaction.

3.1.2. PXRD characterization

The PXRD patterns for the nZVI, MWCNT, and MWCNT-nZVI were illustrated in Fig. 3. For the pure nZVI, the obvious reflection at 2θ of 44.6° was observed to be consistent with zero-valent iron, which belongs to the characteristic peak of α-Fe [44,45], it indicated that the nZVI nanoparticles might either load outside the carbon tubes or inside the pores and cracks of the network [33]. Besides, a very weaker impurity peak of iron oxide (2θ = 35.8°) was observed in the PXRD pattern of MWCNT-nZVI, and it is possible to the formation of iron oxides crystalline phases like Fe_2O_3, Fe_3O_4, and FeOOH [46]. The peak (2θ = 44.6°) of MWCNT-nZVI was weaker and broader compared with nZVI, suggesting that the particle size of iron nanoparticles supported on MWCNT was much smaller than that of nZVI [47]. The characteristics peak (2θ = 25°–27°) of the MWCNT was found in PXRD pattern of MWCNT-nZVI, indicating that MWCNT-nZVI still had type carbon nanotubes structure after supported nZVI.

3.1.3. BET characterization

The N_2 adsorption–desorption isotherms of MWCNT-nZVI and MWCNT composite and pore size distribution curve of MWCNT-nZVI composite (inset) are presented in Fig. 4, the BET surface area, pore volume, and average pore
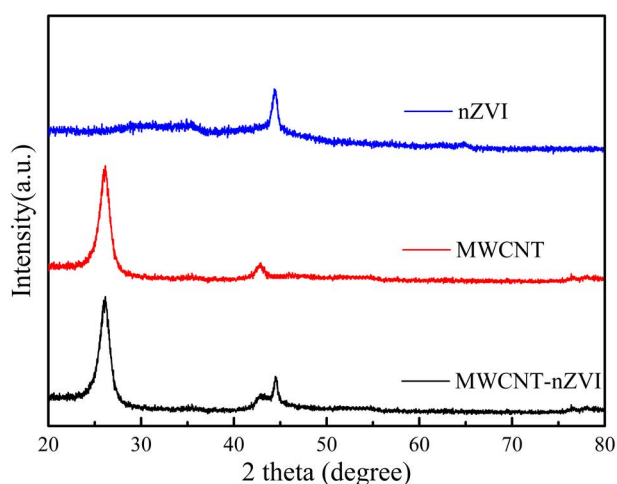

Fig. 3. PXRD pattern of the nZVI, MWCNT, and MWCNT-nZVI.

width of MWCNT-nZVI and MWCNT are listed in Table 2. Recent experiments found that nZVI displayed a typical BET surface area of 54.04 m^2/g [30], and the BET surface area of MWCNT-nZVI and MWCNT are 61.77 and 92.54 m^2/g, which are nearly 1.1 and 1.7 times larger than that of pure nZVI, respectively, suggesting it is suitable for MWCNT to be a support. The average pore size diameter of the MWCNT-nZVI particles increased to 37.19 nm compared to 28.28 nm for MWCNT (Table 2), implying the loading of nZVI did not completely block the transport channels of MWCNT.

According to Fig. 4, based on the International Union of Pure and Applied Chemistry (IUPAC) classification, the kind of isotherm fitted well with the type IV curve of six physisorption isotherms. The previous study has investigated that mesoporous pores range from 2 to 50 nm [48]. It can be considered that the MWCNT-nZVI sample still has a typical mesoporous structure.
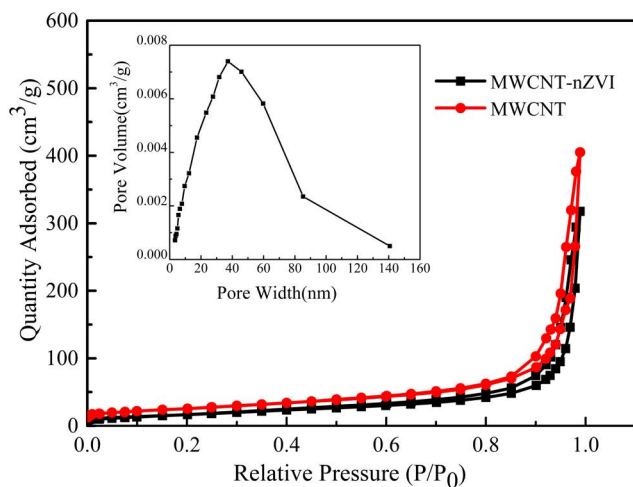
Fig. 4. Nitrogen adsorption–deadsorption isotherms for MWCNT-nZVI and MWCNT composite, pore size distribution curve of MWCNT-nZVI composite (inset).

Table 2
BET surface area and average pore diameter of MWCNT-nZVI and MWCNT composite

Sample	BET surface area (m²/g)	Pore volume (cm³/g)	Average pore width (nm)
MWCNT-nZVI	61.77	0.49	37.19
MWCNT	92.54	0.65	28.28

3.2. Results of the analysis on influencing factors

3.2.1. Effect of temperature

Temperature is an important parameter in the degrading process of PCBs. The dependence of temperature on the removal PCBs by MWCNT-nZVI is observed in Fig. 5a, which can be obviously seen that the removal rate of PCBs increased with reaction temperature was higher, the total reaction was 180 min, the PCBs removal rates under five kinds of temperature were 59.35%, 76.44%, 93.99%, 95.75%, and 97.69% respectively. The reason may be that the rise of temperature can accelerate the molecular motion in the solution, promoting the degradation efficiency of PCBs. Previous studies have reported that the dechlorination reaction was endothermic [49,50]. Therefore, it can promote the removal of PCBs by nZVI though increasing the reaction temperature. Apul and Karanfil [51] considered that the adsorption of SOCs (synthetic organic contaminants) by CNTs (carbon nanotubes) was predominantly a temperature-dependent process. However, how temperature affects the mechanism by which multi-walled carbon nanotubes adsorb PCBs needs further investigation.

The pseudo-first-order kinetics and pseudo-secondary-order kinetics model simulation of the degradation of PCBs by MWCNT-nZVI under different temperature is revealed in Figs. 5b and c, respectively. The kinetics parameter of PCBs remove under different temperature

values is observed in Table 3. The result showed that the R^2 of the linear pseudo-secondary-order kinetics model was higher than 0.9000, which was higher than the result of the pseudo-first-order kinetics model. It illustrates the degradation process of PCBs onto MWCNT-nZVI composites was more in line with the pseudo-secondary-order kinetics model compared to the pseudo-first-order kinetics model. Nevertheless, because the temperature of the sewage treatment plant water is close to 25°C in the summer, and considerate the energy saving, 25°C was chosen as the experimental temperature to investigate the optimal reaction condition.

According to the Arrhenius equation to investigate the temperature effects on the reductive dechlorination reaction process of PCBs, the functional relationship between temperature and rate constants could be described as follows [49]:

$$k = A \times e^{-\frac{E_a}{RT}} \tag{2}$$

where k is the measured rate constant (k is the measured pseudo-secondary-order kinetics model in this study). E_a is the activation energy. A is a frequency factor, R is the universal gas constant (8.314 J/mol/K), and T is the temperature (K). Integrating Eq. (3) resulted in:

$$\ln k = -\frac{E_a}{RT} + \ln A \tag{3}$$

Through Eq. (3) to plot Fig. 6a, observing a plot of ln$k$ vs. 1/T apparent a linear relationship. In this paper, we studied the activation energy for removal of PCBs by MWCNT-nZVI at different temperatures between 15°C and 35°C and calculated to be 129.58 kJ/mol.

Eq. (4) [52] was used to calculate the thermodynamic parameters, enthalpy change ($\Delta H°$, kJ/mol) and entropy change ($\Delta S°$, J/mol/K).

$$\ln\left(\frac{k}{T}\right) = \ln\left(\frac{k_B}{h}\right) - \frac{H}{R} \times \frac{1}{T} + \frac{S}{R} \tag{4}$$

where k_B is the Boltzmann's constant (1.38×10^{-23} J/K), h is the Planck's constant (6.63×10^{-34} J S).

The apparent linear relationship of ln(k/T) and 1/T are shown in Fig. 6b, and values of $\Delta H°$ and $\Delta S°$ were obtained from the slope and intercept of the linear plot of ln(k/T) vs. 1/T, respectively. After calculation, $\Delta H° = 127.10$ kJ/mol, implying that the reaction was endothermic. The value of $\Delta S°$ is –101.17 kJ/(mol K), $\Delta S°$ could reflect the degree of arrangement and complexity of the products compared to the initial reagents, and the proximity of the system to its own thermodynamic equilibrium and the negative value of entropy suggested that enthalpy was driven of the reaction, and implied that the complex products formed in the reductive dechlorination of PCBs were more structured than the initial molecules and more orders might be generated after the reaction [53]. Lv et al. [53] reported that nanoscale zero-valent iron (nZVI) attached on the Fe_3O_4 nanoparticles ($Fe^0@Fe_3O_4$) were prepared and creatively applied in the
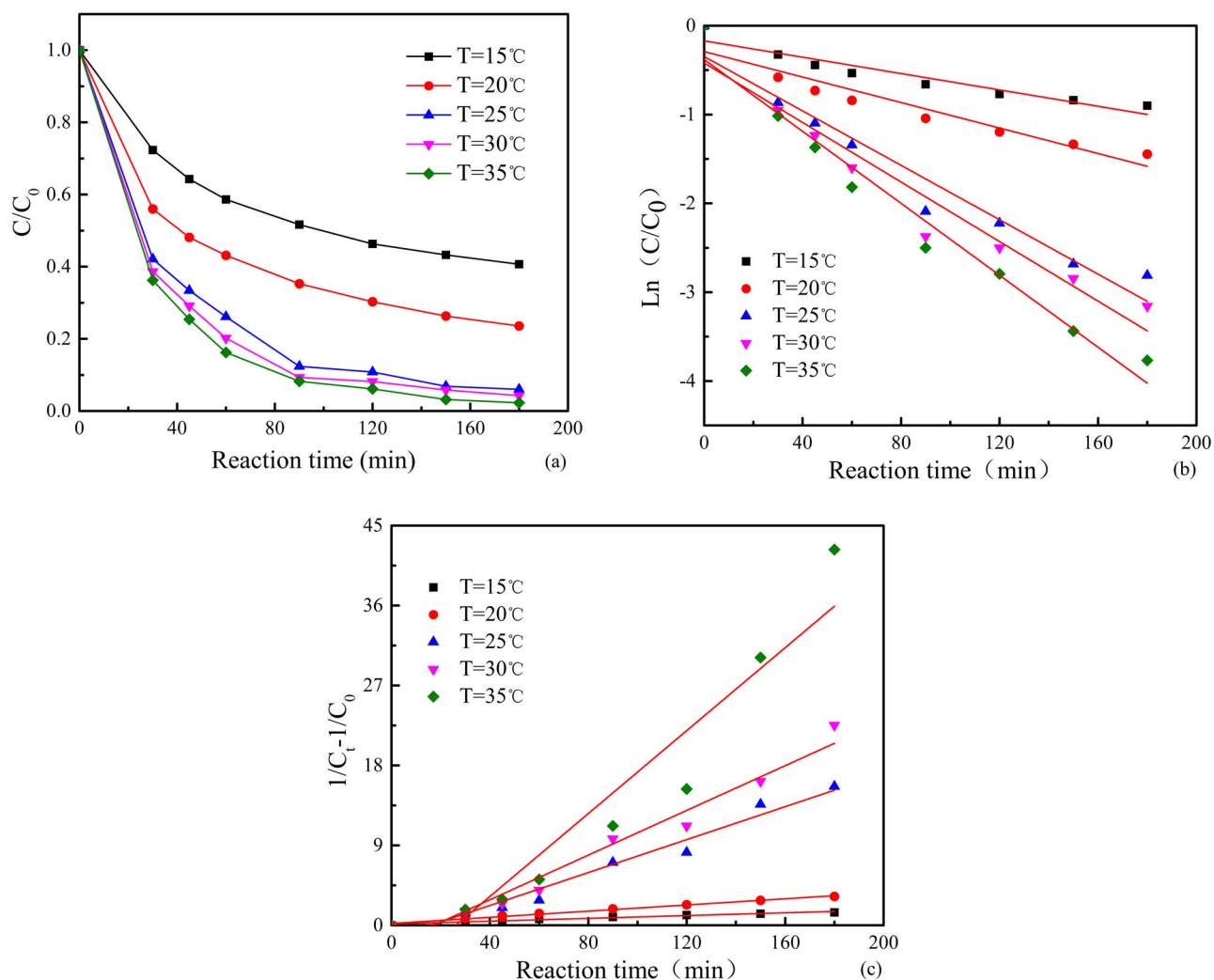
Fig. 5. (a) Effect of temperature on the removal ratio of PCBs, (b) pseudo-first-order kinetics simulation of PCBs degradation under different temperature, and (c) pseudo-secondary-order kinetics simulation of PCBs degradation under different temperature. Initial reaction condition: [PCBs] = 1.4 mg/L, [MWCNT-nZVI] = 1.6 g/L, pH = 7.

Table 3
Kinetics simulation parameter of PCBs remove under different temperature values

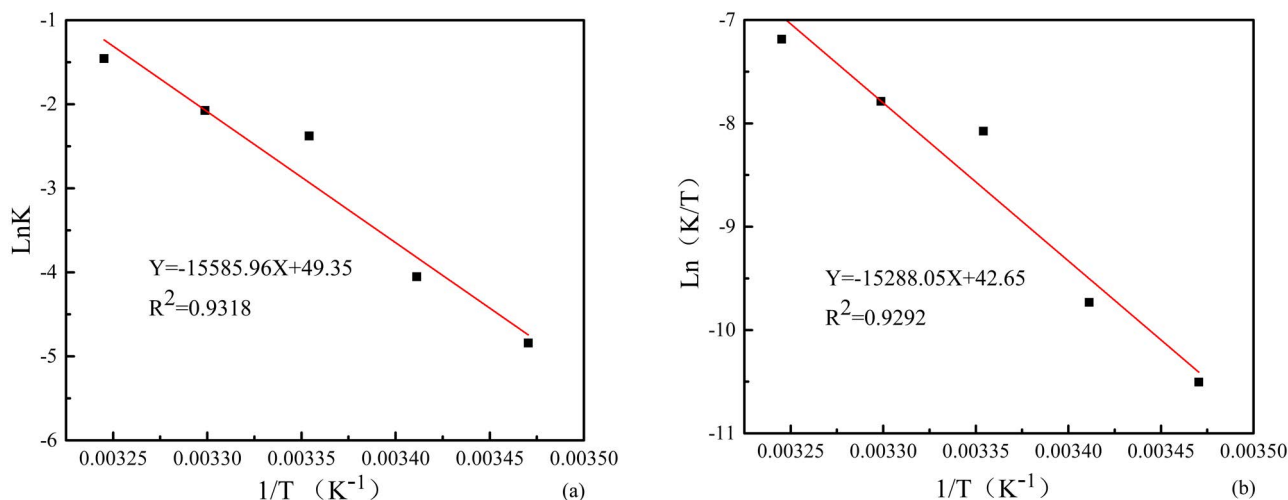| Temperature (°C)	Pseudo-first-order kinetics		Pseudo-secondary-order kinetics	
	K_a (1/min)	R^2	K_a (1/min)	R^2
15	0.0046	0.8905	0.0079	0.9688
20	0.0072	0.8856	0.0174	0.9913
25	0.0153	0.9380	0.0927	0.9669
30	0.0168	0.9278	0.1258	0.9646
35	0.0203	0.9636	0.2334	0.9091

Fig. 6. (a) Fitting curve of lnK/T and (b) fitting curve of ln(K/T)/T.

reductive dechlorination of carbon tetrachloride (CT), and demonstrated that the reaction of removal CT by $Fe^0@Fe_3O_4$ was an endothermic reaction, the reaction of entropy was negative [54].

3.2.2. Effect of MWCNT-nZVI dosage

To analyze the effect of MWCNT-nZVI dosage on the removal ratio of PCBs, and the result is illustrated in Fig. 7a. With the increase of MWCNT-nZVI dosage, the removal efficiency of PCBs was 64.84%, 74.38%, 85.38%, 93.99%, and 95.98%, respectively. The reason was that the dosage of MWCNT-nZVI increase, the total amount and the total surface area of the nZVI involved in the reaction increased, which could make more complete removal of PCBs and provide more free electrons for the reductive dechlorination, resulting in that the removal efficiency of PCBs increased. It is obvious that a relatively low removal rate was obtained with the MWCNT-nZVI dosage of 1.0 g/L, implying a lack of reactive sites. When the MWCNT-nZVI dosage was 2.0 g/L, it implied plenty of reactive sites. Fe^0 is an excellent source of reducing equivalents-serving as the original source of an electron donor such as Fe^{2+} or H_2 [55]. The consumption of a given mass of contaminants only needs the appropriate lots of catalysts, and excessive catalyst will react with water, possibly leading to a larger amount of hydrogen production. The generated H_2 may adhere to the surface of MWCNT-nZVI particles, which are not conducive to the dechlorination of PCBs due to the hindering of the active site [54]. Therefore, it is necessary to choose a more suitable catalyst dosage.

3.2.3. Effect of initial pH

The pH value not only affects the chemical properties of the material but also influences the reaction products and species of formed iron oxides. In order to investigate the effect of pH on removing ratio of PCBs, and the initial pH value was adjusted to 3.0, 5.0, 7.0, 8.5, and 10.0 by H_2SO_4 and NaOH solutions with suitable concentration.

From Fig. 7b, it can be concluded that after 180 min, the removal efficiency reached 70.05%, 85.04%, 93.99%, 49.90%,

and 42.10%, respectively. The result implied that higher efficiency could be achieved in neutral conditions, and with a decrease of pH from 10.0 to 7.0. The following reasons could explain this phenomenon: (1) more H^+ was released at lower pH values, which could not only accelerate the corrosion of nZVI particles, but also eliminated ferrous hydroxide and other passive layers on the surface of the incorporated Fe^0 to generate fresh active sites. Therefore, this will improve the electron transfer from nZVI to PCBs and increase the reduction rate [56,57], (2) alkaline pH could enhance the formation of the iron hydroxide precipitates, which eventually forms a surface layer (or passive film) on the nZVI particles and inhibits further reactions involving direct electron and proton transfers [58].

3.2.4. Effect of initial PCBs concentrations

At presented in Fig. 7c, with the increase of the initial PCBs concentrations, the removal efficiency of PCBs was decreasing. With different initial PCBs concentrations, finally removal efficiency of PCBs reached 98.00%, 93.99%, 70.69%, and 54.99%, respectively. When the initial concentration was 0.7 mg/L, finally removal efficiency of PCBs was close to 99%, which was close to the removal efficiency of PCBs in the initial concentration of 1.4 mg/L, which indicated that the active site may be adequate. On the contrary, there was not enough active site in the process of 2.1 and 2.8 mg/L initial PCBs concentrations. Therefore, the final removal efficiency of PCBs was lower. Recent evidence suggests that the limited active sites could become a constraint factor that obstructed continuous reaction with a gradually decreased reaction rate [53], this phenomenon could be explained by it.

In a word, through experimental research, the temperature was 25°C, and the pH was 7.0, which were the optimum reaction conditions.

3.3. Mechanism analysis

When the initial PCBs were 1.4 mg/L, T = 25°C, and pH = 7.0, with nZVI, MWCNT-nZVI, and MWCNT dosage
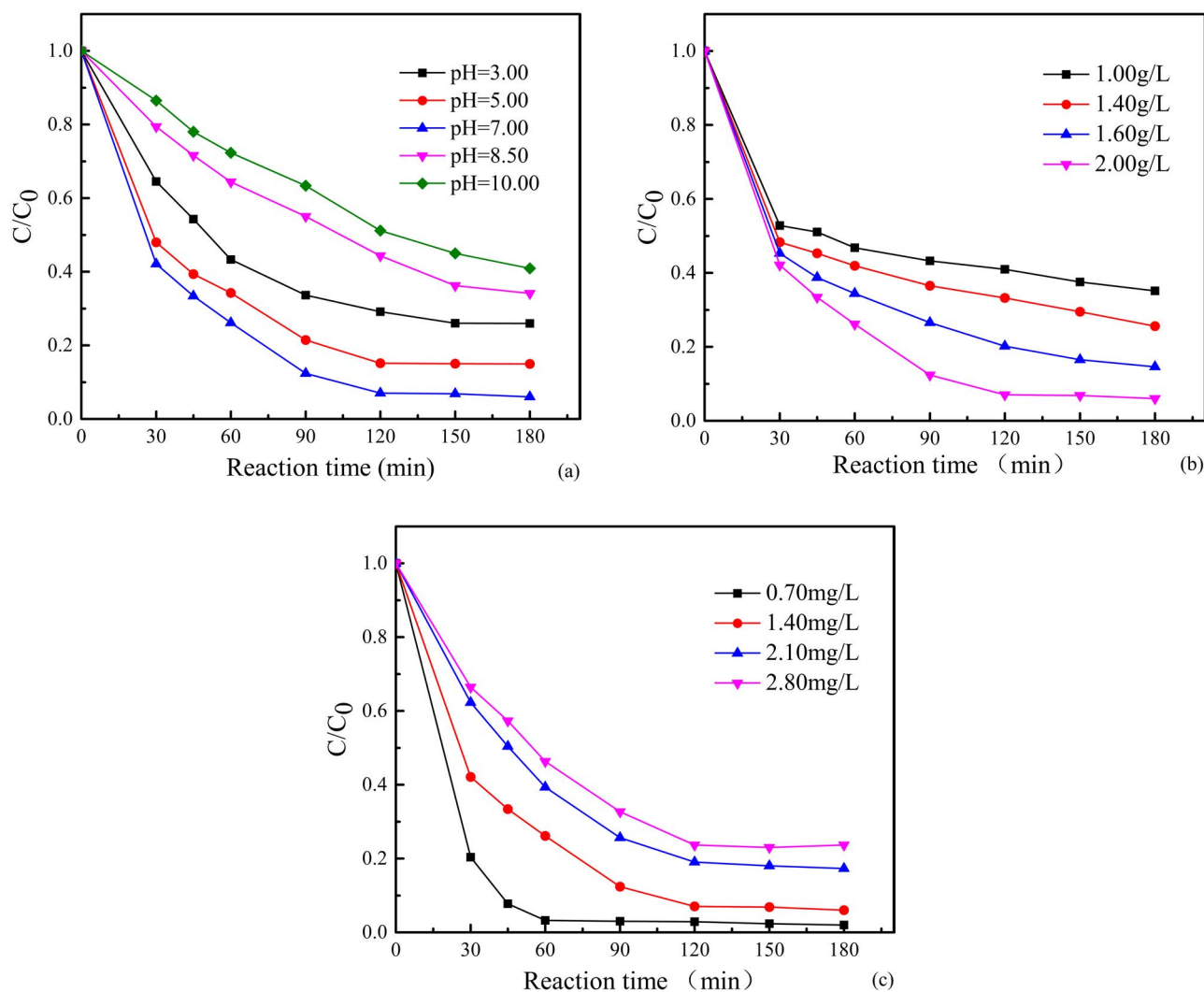
Fig. 7. (a) Effect of MWCNT-nZVI dosage on removal ratio of PCBs, (b) effect of pH on removal ratio of PCBs, and (c) effect of initial PCBs concentrations on removal ratio of PCBs. Initial reaction condition: [PCBs] = 1.4 mg/L(a and c), [MWCNT-nZVI] = 1.6 g/L (a and b), pH = 7 (b and c), T = 25°C (a–c).

of 1.0 g/L, the removal efficiency curves of nZVI, MWCNT-nZVI, and MWCNT were shown and compared in Fig. 8a. The content of PCBs without any adsorbent material was basically unchanged, and the PCBs content decreased only 1.72% at the end of the reaction, which proved that the liquid-phase PCBs in the experimental process was basically free of volatilization or self-degradation. During the first hour of reaction, the content of PCBs in all groups decreased significantly, and the removal rate of PCBs was more than 50% except nZVI. The removal rate of MWCNT (57.53%) was only slightly higher than MWCNT-nZVI (53.21%), but the removal efficiency of nZVI only was 20%. Recently investigators have found that the specific surface area plays a certain role in the total removal rate of pollutants in the initial stage of the reaction [59,60]. According to the BET test results in Table 2, the loading of nZVI makes the specific surface area and pore volume of MWCNT-nZVI slightly smaller than MWCNT's, therefore MWCNT may have a slightly better effect on liquid-phase PCBs removal during

the first 1 h. When the reaction proceeded to 6 h, the adsorption of PCBs by MWCNTs was basically balanced, and the MWCNT-nZVI materials still had the tendency to continue to remove PCBs. After 6 h of reaction, the removal efficiency of PCBs by nZVI, MWCNT-nZVI, and MWCNT were 41.18%, 71.94%, and 63.84%, respectively. It is suggested that the chemical dechlorination reaction compensates for the disadvantage of the reduced specific surface area resulting in insufficient adsorption and makes the MWCNT-nZVI composite exhibit better removal ability for PCBs. The bad dispersions of nZVI may cause low removal efficiency of PCBs [27,61].

It can be seen that the pseudo-first-order kinetics model and pseudo-secondary-order kinetics equation fit the removal process of PCBs by nZVI, MWCNT-nZVI, and MWCNT from Figs. 8b and c and Table 4, and the fitting results showed a good linear relationship. The correlation coefficient R^2 was all higher than 0.80. However, the result of the pseudo-secondary-order kinetics equation fits
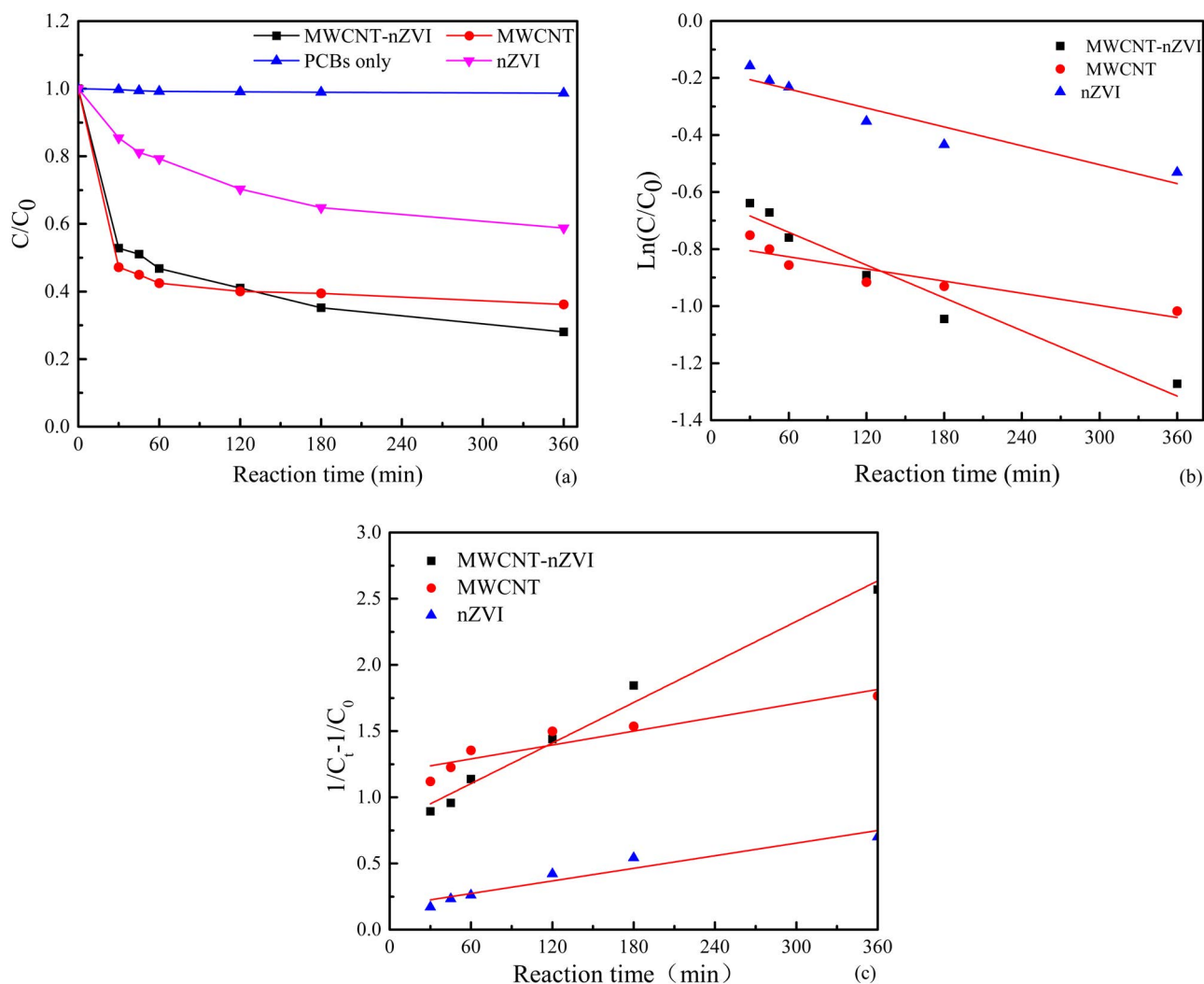
Fig. 8. (a) Comparison between different catalysts on degradation of PCBs, (b) pseudo-first-order kinetics equation fitting curve for the removal of PCBs, and (c) pseudo-secondary-order kinetics equation fitting curve for the removal of PCBs (reaction condition: [PCBs] = 1.4 mg/L, [nZVI] = 1.0 g/L, [MWCNT] = 1.0 g/L, [MWCNT-nZVI] = 1.0 g/L, PH = 7.0, and T = 25°C).

Table 4
Parameter of kinetic model of PCBs remove by MWCNT-nZVI and MWCNT

Catalysts	Pseudo-first-order kinetics		Pseudo-secondary-order kinetics	
	K_a (1/min)	R^2	K_a (1/min)	R^2
nZVI	0.0011	0.8789	0.0016	0.9110
MWCNT	0.0007	0.8091	0.0018	0.8440
MWCNT-nZVI	0.0019	0.9467	0.0051	0.9813

is better than the pseudo-first-order kinetics model. The pseudo-secondary-order kinetics rate constant of MWCNT-nZVI is 2.83 times than MWCNT's. This may be the location of the dechlorination reaction mainly occurs on the surface of MWCNT-nZVI [49,50], and the adsorption of MWCNT increases the content of PCBs near nZVI, so, which enhances the pseudo-secondary-order kinetics rate constant of MWCNT-nZVI.

The experiments of MWCNT and MWCNT-nZVI removal PCBs were carried out for 17 h, and the removal rates reached 71% and 87%, respectively. The balance mass of PCBs in the liquid-phase and of MWCNT solid-phase was calculated. It is presented in Fig. 9a. In the past decade, many researchers have determined that MWCNT is an excellent adsorbent [20,21,31]. The presence of Cl⁻ was not detected in the liquid-phase, indicating that there was no dechlorination
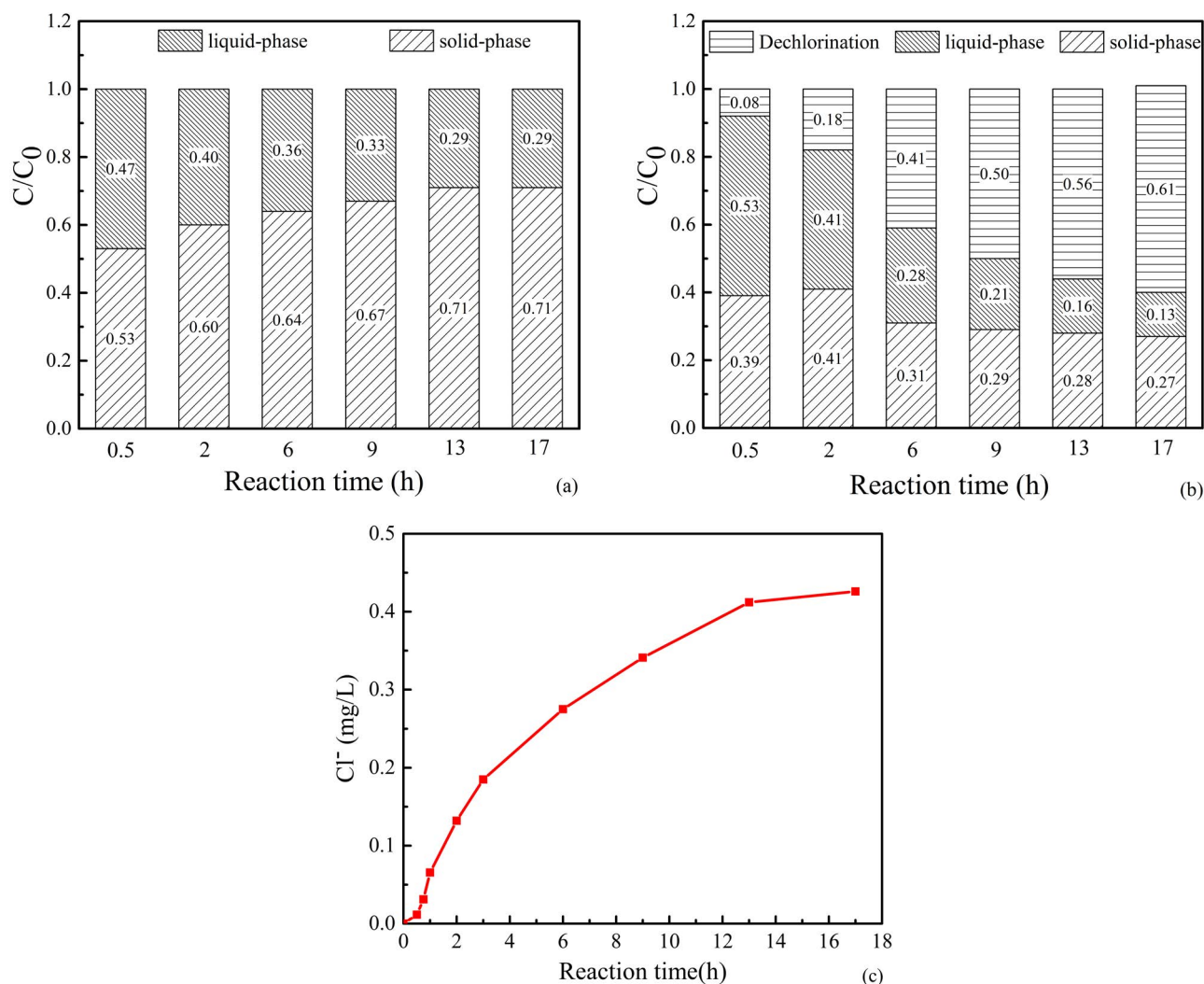
Fig. 9. (a) Mass balance calculation of PCBs removal using MWCNT, (b) mass balance calculation of PCBs removal using MWCNT-nZVI (reaction condition: [PCBs] = 1.4 mg/L, [MWCNT] = 1.0 g/L, [MWCNT-nZVI] = 1.0 g/L, PH = 7.0, and T = 25°C), and (c) chloride ion content variation in the process of MWCNT-nZVI removing PCBs.

of PCBs in this process, and this is just an adsorption removal process. On the contrary, from Figs. 9b and c, 2 h before the reaction, the outer surface of the MWCNT provided a lot of active sites, the PCBs were quickly adsorbed to the outer surface. So the adsorption rate was faster. The contact time of nZVI with PCBs is later than the adsorption time of MWCNT-nZVI material, the rate of reductive dechlorination is slower, and the adsorption rate of PCBs is higher than that of dechlorination. Therefore, solid-phase PCBs are accumulated [62]. After 2 h of reaction, the PCBs that were adsorbed on the solid-phase began to decrease. At this time, nZVI accelerated the reduction of PCBs adsorbed onto the solid-phase. Although MWCNT-nZVI can continue to adsorb PCBs from the liquid-phase, the adsorption rate at this time is less than the rate of reductive dechlorination, resulting in a continuous reduction in solid-phase PCBs.

The mechanism of PCBs dechlorinated by nZVI has been explored by many researchers. The following two methods are widely accepted by researchers. As shown in Fig. 10, first,

PCBs as an electron acceptor to react with nZVI, and nZVI reacts directly with PCBs in the dechlorination process [63]. Second, the electron was moved from nZVI to H_2O, firstly. The generated hydrogen could complete the reactivity with organic chloride [64]. All these above paths coexisted in our system and were dominated by the first paths. As Fig. 7b displays, higher efficiency can be achieved in neutral conditions. Experiments at different initial pH values were conducted, and the final pH values were measured. As shown in Table 5, a certain increase in pH value occurred under neutral conditions, whereas slight increases were found under alkaline and acidic conditions. When the initial pH value is 5.0 and 7.0, the final pH values increased to 5.2 and 7.4 after reaction over, respectively. The PCBs removal efficiency when pH is 5.0 is lower than pH is 7.0. It implied that nZVI reacted directly with PCBs in the dechlorination process, the first path dominant in the reaction.

Exploring through experiment, the chemical reaction equation for reductive dechlorination is as follows:

Table 5
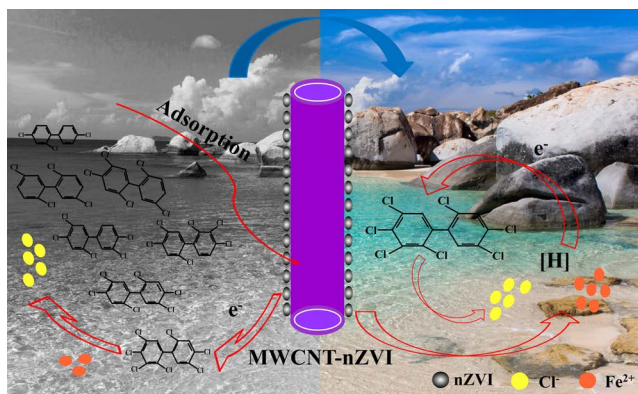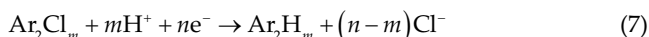Changes in solution pH values

Initial pH	3.0	5.0	7.0	8.5	10.0
Final pH	3.1	5.2	7.4	8.7	10.1

Fig. 10. Adsorption and reduction mechanism of PCBs by MWCNT-nZVI.

$$Fe^0 \rightarrow Fe^{2+} + 2e^- \tag{6}$$

$$Ar_2Cl_m + mH^+ + ne^- \rightarrow Ar_2H_m + (n-m)Cl^- \tag{7}$$

In the MWCNT-nZVI composite system, MWCNT can effectively adsorb the mass transfer [33], while nZVI is mainly responsible for providing electrons. As a carrier, MWCNT aggregates PCBs in the liquid-phase around nZVI, increasing the contact of nZVI with target contaminants, and improving the dechlorination reduction effect of nZVI on PCBs.

Dechlorination of PCBs can also be manifested by the concentration of Cl$^-$ and is shown in Fig. 9c. As the reaction time increases, the Cl$^-$ concentration increases continuously, indicating that the reductive dechlorination process continues continuously. The dechlorination efficiency of PCBs was calculated by using the detected Cl$^-$ concentration and compared with the theoretical value. It was found that the actual dechlorination efficiency was slightly lower than the theoretical value, and the error was 0.32% to 6.98%. Previous studies have reported that a bit of Cl$^-$ may adsorb on the iron hydroxide product, and resulting in a decrease in Cl$^-$ concentration [65].

For the process of the nZVI removing PCBs, many researchers studied that non-ortho-substituted congeners had faster initial dechlorination rates than ortho-substituted congeners in the same homolog group [16]. Seven different PCBs (PCB28, PCB52, PCB101, PCB118, PCB138, PCB153, and PCB180,) were used to investigate the rule of PCBs dechlorination in experiments. It can obviously study that PCBs with higher chlorine atoms were firstly removed. The concentration of PCBs with lower chlorine atoms was elevated as PCBs with higher chlorine atoms decline. However, it is hard to recognize the rule of PCBs dechlorination, because the product of dechlorination is difficult to determine.
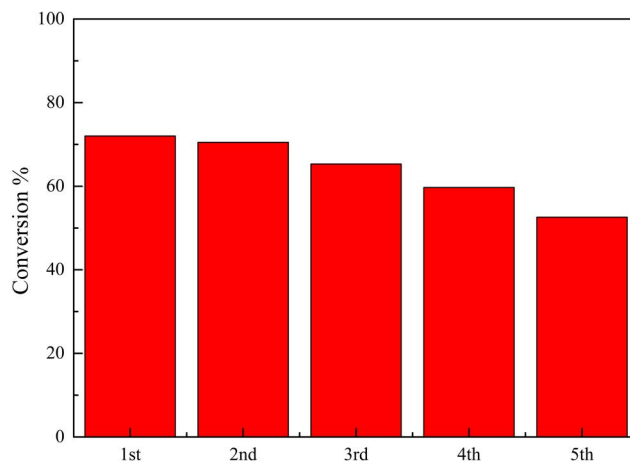

Fig. 11. Cyclic performance of PCBs reduction over MWCNT-nZVI.

3.4. Reusability and stability of MWCNT-nZVI

Regeneration and stability of the MWCNT-nZVI composite for the removal of PCBs from water are also important properties for the evaluation of its practical use performance. This study also investigated the reusability of MWCNT-nZVI for PCBs treatment. Regeneration of the MWCNT-nZVI composite should be attained by washing and oscillation treatment [66]. After the first cycle, the used MWCNT-nZVI particles were regenerated by washing them with 0.01 M HCl to remove the oxide layer and to dissolve the precipitated iron and chloride [61,67]. The particles then were washed with *n*-hexane and ultra-pure water and dried under the vacuum overnight. As depicted in Fig. 11, the PCBs degradation efficiency decreased from 71.94% to 52.60% after five cycles, illustrating that MWCNT-nZVI could be reusable. After reusing five times, the removal efficiency of PCBs dropped 19.34%. The main reason was that the loss of nZVI increased with the increase of the cycle of reuse [68].

4. Conclusions

In this research, MWCNT was chosen as a dispersant and supporter to immobilize nZVI. MWCNT-nZVI was successfully prepared by a liquid-phase reduction reaction and applied in the dechlorination of PCBs firstly. Compared with MWCNT, pure nZVI, and MWCNT-nZVI could reach a high degradation efficiency MWCNT-nZVI can overcome the aggregation and surface passivation problem of nZVI, and enhance the activity and stability of nZVI. The PCBs removal efficiency of MWCNT-nZVI reached 71.94% in 6 h. It was higher than MWCNT (8.1%) and n-ZVI (30.76%), respectively. The removal process obeyed the pseudo-secondary-order kinetics model. By calculating the material balance of Cl$^-$ during the degradation of PCBs by MWCNT-nZVI, it demonstrated that MWCNT-nZVI has not only a reduction effect but also an adsorption effect on PCBs. The reduction activity of nZVI was efficiently supported by MWCNT, which can accelerate electrons transfer in the composite and greatly enhance the reduction

activity of nZVI. Besides, two reaction pathways for PCB removal by n-ZVI were proposed. Our research provides a fast and easily available modified catalyst for degrading PCBs in the environment. The future research direction needs to research and verify the degradation intermediates of PCBs by electron paramagnetic resonance (EPR) technique, gas chromatography/mass spectrometer (GC-MS) and improves the degradation efficiency of PCBs in water by supporting Fe and Pd to MWCNT.

Acknowledgment

References

[1] S. Safe, O. Hutzinger, Polychlorinated biphenyls (PCBs) and polybrominated biphenyls (PBBs): biochemistry, toxicology, and mechanism of action, Crit. Rev. Toxicol., 13 (1984) 319–395.

[2] Y.A. Shaban, M.A.E. Sayed, A.A.E. Maradny, R.K.A. Farawatia, M.I.A. Zobidi, S.U.M. Khanc, Photocatalytic removal of polychlorinated biphenyls (PCBs) using carbon-modified titanium oxide nanoparticles, Appl. Surf. Sci., 365 (2016) 108–113.

[3] K.C. Jones, P.D. Voogt, Persistent organic pollutants (POPs): state of the science, Environ. Pollut., 100 (1999) 209–221.

[4] Y. Abrha, D. Raghavan, Polychlorinated biphenyl (PCB) recovery from spiked organic matrix using accelerated solvent extraction (ASE) and Soxhlet extraction, J. Hazard. Mater., 80 (2000) 147–157.

[5] K. Anezaki, T. Nakano, Unintentional PCB in chlorophenylsilanes as a source of contamination in environmental samples, J. Hazard. Mater., 287 (2015) 111–117.

[6] K. Anezaki, T. Nakano, Concentration levels and congener profiles of polychlorinated biphenyls, pentachlorobenzene, and hexachlorobenzene in commercial pigments, Environ. Sci. Pollut. Res., 21 (2014) 998–1009.

[7] J.D. Hutchinson, M.P. Simmonds, Organochlorine contamination in pinnipeds, Rev. Environ. Contam. Toxicol., 136 (1994) 123–167.

[8] W. Brack, T. Kind, H. Hollert, S. Schraderc, M. Möderc, Sequential fractionation procedure for the identification of potentially cytochrome P4501A-inducing compounds, J. Chromatogr. A, 986 (2003) 55–66.

[9] C. Bergkvist, M. Kippler, S.C. Larsson, M. Berglund, A. Glynn, A. Wolk, A. Kesson, Dietary exposure to polychlorinated biphenyls is associated with increased risk of stroke in women, J. Intern. Med., 276 (2015) 248–259.

[10] R.F. Marek, P.S. Thorne, D.W. Jeanne, K.C. Hornbuckle, Variability in PCB and OH-PCB serum levels in children and their mothers in urban and rural U.S. communities, Environ. Sci. Technol., 48 (2014) 13459–13467.

[11] E.H. Buckley, Accumulation of airborne polychlorinated biphenyls in foliage, Science, 216 (1982) 520–522.

[12] Y. Mahfooz, A. Yasar, M.T. Sohail, A.B. Tabinda, R. Rasheed, S. Irshad, B. Yousaf, Investigating the drinking and surface water quality and associated health risks in a semi-arid multi-industrial metropolis (Faisalabad), Pakistan, Environ. Sci. Pollut. Res., 26 (2019) 20853–20865.

[13] M.T. Sohail, R. Aftabb, Y. Mahfoozc, A. Yasar, Y. Yen, S.A. Shaikh, S. Irshad, Estimation of water quality, management and risk assessment in Khyber Pakhtunkhwa and Gilgit-Baltistan, Pakistan, Desal. Water Treat., 171 (2019) 105–114.

[14] M.T. Sohail, Y. Mahfoozb, K. Azamc, Y. Yen, G.F. Liao, S. Fahad, Impacts of urbanization and land cover dynamics on underground water in Islamabad, Pakistan, Desal. Water Treat., 1159 (2019) 402–411.

[15] B. Gelavizh, J. Sahand, V. Zarezade, M. Khatebasreh, F. Mehdipour, F. Ghanbari, 4-Chlorophenol degradation using ultrasound/peroxymonosulfate/nanoscale zero valent iron: reusability, identification of degradation intermediates and potential application for real wastewater, Chemosphere, 201 (2018) 370–379.

[16] G.V. Lowry, K.M. Johnson, Congener-specific dechlorination of dissolved PCBs by microscale and nanoscale zerovalent iron in a water/methanol solution, Environ. Sci. Technol., 38 (2004) 5208–5216.

[17] S.Q. Wang, C. Chen, S.Y. Zhao, J.Z. He, Microbial synergistic interactions for reductive dechlorination of polychlorinated biphenyls, Sci. Total Environ., 666 (2019) 368–376.

[18] L. Xu, Y. Teng, Z.G. Li, M. Norton, Y.M. Luo, Enhanced removal of polychlorinated biphenyls from alfalfa rhizosphere soil in a field study: the impact of a rhizobial inoculum, Sci. Total Environ., 408 (2010) 1007–1013.

[19] J. Borja, D.M. Taleon, J. Auresenia, S. Gallardo, Polychlorinated biphenyls and their biodegradation, Process Biochem., 40 (2005) 1999–2013.

[20] I. Velzeboer, C.J.A.F. Kwadijk, A.A. Koelmans, Strong sorption of PCBs to nanoplastics, microplastics, carbon nanotubes, and fullerenes, Environ. Sci. Technol., 48 (2014) 4869–4876.

[21] D.D. Shao, G.D. Sheng, C.L. Chen, X.K. Wang, M. Nagatsu, Removal of polychlorinated biphenyls from aqueous solutions using β-cyclodextrin grafted multiwalled carbon nanotubes, Chemosphere, 79 (2010) 679–685.

[22] H. Dudasova, J. Derco, L. Sumegova, K. Dercova. K. Laszlova, Removal of polychlorinated biphenyl congeners in mixture Delor 103 from wastewater by ozonation vs/and biological method, J. Hazard. Mater., 321 (2017) 54–61.

[23] B.Z. Wu, H.Y. Chen, S.J. Wang, C.M. Wai, W.S. Liao, K.H. Chiu, Reductive dechlorination for remediation of polychlorinated biphenyls, Chemosphere, 88 (2012) 757–768.

[24] Z. Liu, F.S. Zhang, Nano-zerovalent iron contained porous carbons developed from waste biomass for the adsorption and dechlorination of PCBs, Bioresour. Technol., 101 (2010) 2562–2564.

[25] R.W. Gillham, S.F.O. Hannesin, Enhanced degradation of halogenated aliphatics by zero-valent iron, Ground Water, 32 (1994) 958–967.

[26] S. Comba, A.D. Molfetta, R. Sethi, A comparison between field applications of nano-, micro-, and millimetric zero-valent iron for the remediation of contaminated aquifers, Water Air Soil Pollut., 215 (2011) 595–607.

[27] M.C. Biesinger, B.P. Payne, A.P. Grosvenor, L.W.M. Lau, A.R. Gerson, R.S.C. Smart, Resolving surface chemical states in XPS analysis of first row transition metals, oxides and hydroxides: Cr, Mn, Fe, Co and Ni, Appl. Surf. Sci., 257 (2011) 2717–2730.

[28] Y. Liu, G.V. Lowry, Effect of particle age (Fe^0 content) and solution pH on NZVI reactivity: H_2 evolution and TCE dechlorination, Environ. Sci. Technol., 40 (2006) 6085–6090.

[29] L. Chekli, B. Bayatsarmadi, R. Sekine, B. Sarkar, A.M. Shen, K.G. Scheckel, W. Skinner, R. Naidu, H.K. Shon, E. Lombi, E. Donner, Analytical characterisation of nanoscale zero-valent iron: a methodological review, Anal. Chim. Acta, 903 (2016) 13–35.

[30] C. Uezuem, T. Shahwan, A.E. Eroglu, K.R. Hallam, T.B. Scott, I. Lieberwirth, Synthesis and characterization of kaolinite-supported zero-valent iron nanoparticles and their application for the removal of aqueous Cu^{2+} and Co^{2+} ions, Appl. Clay Sci., 43 (2009) 172–181.

[31] A.F. Alkaim, Z. Sadik, D.K. Mahdi, S.M. Alshrefi, A.M.A. Sammarraie, F.M. Alamgir, P.M. Singh, A.M. Aljeboree, Preparation, structure and adsorption properties of synthesized multiwall carbon nanotubes for highly effective removal of Maxilon blue dye, Korean J. Chem. Eng., 32 (2015) 2456–2462.

[32] A.A. Markadeh, A. Rezaee, S.O. Rastegar, H. Hossini, S. Ahmadi, E. Hoseinzadeh, Optimization of Remazol Brilliant blue adsorption process from aqueous solutions using multi-walled carbon nanotube, Desal. Water Treat., 57 (2016) 1–9.

[33] X.S. Lv, J. Xu, G.M. Jiang, X.H. Xu, Removal of chromium(VI) from wastewater by nanoscale zero-valent iron particles supported on multiwalled carbon nanotubes, Chemosphere, 85 (2011) 1204–1209.

[34] A. Soliemanzadeh, M. Fekri, Synthesis of clay-supported nanoscale zero-valent iron using green tea extract for the removal of phosphorus from aqueous solutions, Chin. J. Chem. Eng., 25 (2011) 924–930.

[35] Y. Chen, Z.H. Lin, R.G. Hao, H. Xu, C.Y. Huang, Rapid adsorption and reductive degradation of Naphthol Green B from aqueous solution by polypyrrole/attapulgite composites supported nanoscale zero-valent iron, J. Hazard. Mater., 371 (2019) 8–17.

[36] W. Wang, M.H. Zhou, M. Qing, J.J. Yue, X. Wang, Novel NaY zeolite-supported nanoscale zero-valent iron as an efficient heterogeneous Fenton catalyst, Catal. Commun., 11 (2010) 937–941.

[37] J.N. Xiao, B.Y. Gao, Q.Y. Yue, Y. Gao, Q. Li, Removal of trihalomethanes from reclaimed-water by original and modified nanoscale zero-valent iron: characterization, kinetics and mechanism, Chem. Eng. J., 262 (2015) 1226–1236.

[38] T. Liu, Z.L. Wang, Y. Sun, Manipulating the morphology of nanoscale zero-valent iron on pumice for removal of heavy metals from wastewater, Chem. Eng. J., 263 (2015) 55–61.

[39] X. Zhang, S. Lin, X.Q. Lu, Z.L. Chen, Removal of Pb(II) from water using synthesized kaolin supported nanoscale zero-valent iron, Chem. Eng. J., 163 (2010) 243–248.

[40] H. Feng, D.Y. Zhao, C. Roberts, Stabilization of zero-valent iron nanoparticles for enhanced *in situ* destruction of chlorinated solvents in soils and groundwater, Nanotechnol. Appl. Clean Water, 31 (2014) 491–501.

[41] X. Zhang, S. Lin, Z.L. Chen, M. Megharaj, R. Naidu, Kaolinite-supported nanoscale zero-valent iron for removal of Pb from aqueous solution: reactivity, characterization and mechanism, Water Res., 45 (2011) 3481–3488.

[42] L.N. Shi, X. Zhang, Z.L. Chen, Removal of chromium(VI) from wastewater using bentonite-supported nanoscale zero-valent iron, Water Res., 45 (2011) 890–892.

[43] J.A. Gyamfi, V. Acha, Carriers for nano zerovalent iron (nZVI): synthesis, application and efficiency, RSC Adv., 6 (2016) 91025–91044.

[44] E. Petala, K. Dimos, A. Douvalis, T. Bakas, J. Tucek, R. Zboril, M.A. Karakassides, Nanoscale zero-valent iron supported on mesoporous silica: characterization and reactivity for Cr(VI) removal from aqueous solution, J. Hazard. Mater., 261 (2013) 295–306.

[45] Z.Q. Fang, X.H. Qiu, J.H. Chen, X.Q. Qiu, Debromination of polybrominated diphenyl ethers by Ni/Fe bimetallic nanoparticles: influencing factors, kinetics, and mechanism, J. Hazard. Mater., 185 (2011) 958–969.

[46] Y.P. Sun, X.Q. Li, J.H. Cao, W.X. Zhang, H.P. Wang, Characterization of zero-valent iron nanoparticles, Adv. Colloid Interface Sci., 120 (2006) 47–56.

[47] Z.H. Pang, M.Y. Yan, X.S. Jia, Z. X. Wang, J.Y. Chen, Debromination of decabromodiphenyl ether by organo-mont-morillonitesupported nanoscale zero-valent iron: preparation, characterization and influence factors, J. Environ. Sci., 26 (2014) 483–491.

[48] M. Kruk, M. Jaroniec, Gas adsorption characterization of ordered organic–inorganic nanocomposite materials, Chem. Mater., 13 (2001) 3169–3183.

[49] X.F. Lv, H. Li, Y.Y. Ma, H. Yang, Q. Yang, Degradation of carbon tetrachloride by nanoscale zero-valent iron@magnetic Fe_3O_4: impact of reaction condition, kinetics, thermodynamics and mechanism, Appl. Organomet. Chem., 32 (2018) e4139.

[50] J.J. Wei, X.H. Xu, Y. Liu, D.H. Wang, Catalytic hydrodechlorination of 2,4-dichlorophenol over nanoscale Pd/Fe: reaction pathway and some experimental parameters, Water Res., 40 (2006) 348–354.

[51] O.G. Apul, T. Karanfil, Adsorption of synthetic organic contaminants by carbon nanotubes: a critical review, Water Res., 68 (2015) 34–55.

[52] L.L. Fan, C.N. Luo, M. Sun, X.J. Li, H.M. Qiu, Highly selective adsorption of lead ions by water-dispersible magnetic chitosan/graphene oxide composites, Colloids Surf., B, 103 (2013) 523–529.

[53] X.F. Lv, X.Q. Xue, G.M. Jiang, D.L. Wu, T.T. Sheng, H.Y. Zhou, X.H. Xu, Nanoscale zero-valent iron (nZVI) assembled on magnetic Fe_3O_4/graphene for chromium(VI) removal from aqueous solution, J. Colloid Interface Sci., 417 (2014) 51–59.

[54] Y.W. Wu, Q.Y. Yue, Z.F. Ren, B.Y. Gao, Immobilization of nanoscale zero-valent iron particles (nZVI) with synthesized activated carbon for the adsorption and degradation of chloramphenicol (CAP), J. Mol. Liq., 262 (2018) 19–28.

[55] B.D. Yirsaw, M. Megharaj, Z.L. Chen, N. Ravi, Environmental application and ecological significance of nano-zero valent iron, J. Environ. Sci., 44 (2016) 88–98.

[56] A. Agrawal, P.G. Tratnyek, Reduction of nitro aromatic compounds by zero-valent iron metal, Environ. Sci. Technol., 30 (1996) 153–160.

[57] M.P. Watts, V.S. Coker, S.A. Parry, R.A.D. Thomas, R. Kalin, J.R. Lliyd, Biogenic nano-magnetite and nano-zero valent iron treatment of alkaline Cr(VI) leachate and chromite ore processing residue, Appl. Geochem., 54 (2015) 27–42.

[58] X.G. Li, Y. Zhao, B.D. Xi, X.G. Meng, B. Gong, R. Li, X. Peng, H.L. Liu, Decolorization of methyl orange by a new clay-supported nanoscale zero-valent iron: Synergetic effect, efficiency optimization and mechanism, J. Environ. Sci., 52 (2017) 8–17.

[59] W. Zhang, T. Yu, X.L. Han, W.C. Ying, Removal of 2-ClBP from soil–water system using activated carbon supported nanoscale zerovalent iron, J. Environ. Sci., 47 (2016) 143–152.

[60] H. Choi, R. Souhail A. Abed, S. Agarwal, D.D. Dionysiou, Synthesis of reactive nano-Fe/Pd bimetallic system-impregnated activated carbon for the simultaneous adsorption and dechlorination of PCBs, Chem. Mater., 20 (2015) 3649–3655.

[61] M. Soroosh, A. Hyeunhwan, C. Dongwon, J. Moon, Activated carbon impregnated by zero-valent iron nanoparticles (AC/nZVI) optimized for simultaneous adsorption and reduction of aqueous hexavalent chromium: material characterizations and kinetic studies, Chem. Eng. J., 353 (2018) 781–795.

[62] C. Hyeok, A. Shirish, S.R. Al-Abed, Adsorption and simultaneous dechlorination of PCBs on GAC/Fe/Pd: mechanistic aspects and reactive capping barrier concept, Environ. Sci. Technol., 43 (2009) 488–493.

[63] L.J. Matheson, P.G. Tratnyek, Reductive dehalogenation of chlorinated methanes by iron metal, Environ. Sci. Technol., 28 (1994) 2045–2053.

[64] R. Lookman, L. Bastiaens, B. Borremans, M. Maesen, J. Gemoets, L. Diels, Batch-test study on the dechlorination of 1,1,1-trichloroethane in contaminated aquifer material by zero-valent iron, J. Contam. Hydrol., 74 (2004) 133–144.

[65] R.J. Barnes, O. Riba, M.N. Gardner, T.B. Scott, S.A. Jackman, I.P. Thompson, Optimization of nano-scale nickel/iron particles for the reduction of high concentration chlorinated aliphatic hydrocarbon solutions, Chemosphere, 79 (2010) 448–454.

[66] H. Xu, W.G. Tian, Y.J. Zhang, J. Tang, Z.T. Zhao, Y. Chen, Reduced graphene oxide/attapulgite-supported nanoscale zero-valent iron removal of acid red 18 from aqueous solution, Water Air Soil Pollut., 229 (2018) 229–238.

[67] X.Y. Li, L.H. Ai, J. Jiang, Nanoscale zerovalent iron decorated on graphene nanosheets for Cr(VI) removal from aqueous solution: surface corrosion retard induced the enhanced performance, Chem. Eng. J., 288 (2016) 789–797.

[68] H. Xu, Y.J. Zhang, Y. Cheng, T. Yong, W.G. Zhao, Z.T. Tang, J. Jiang, Polyaniline/attapulgite-supported nanoscale zero-valent iron for the rival removal of azo dyes in aqueous solution, Adsorpt. Sci. Technol., 37(1019) 217–235.